

## Muon-Spin-Relaxation Investigation of $\text{EuMn}_2\text{O}_5$

S. I. Vorob'ev<sup>a,\*</sup>, E. I. Golovenchits<sup>b</sup>, V. P. Koptev<sup>a</sup>, E. N. Komarov<sup>a</sup>,  
S. A. Kotov<sup>a</sup>, V. A. Sanina<sup>b</sup>, and G. V. Shcherbakov<sup>a</sup>

<sup>a</sup> Petersburg Nuclear Physics Institute, Russian Academy of Sciences, Gatchina, 188300 Russia

\* e-mail: vsiloa@pnpi.spb.ru

<sup>b</sup> Ioffe Physicotechnical Institute, Russian Academy of Sciences,  
Politekhnicheskaya ul. 26, St. Petersburg, 194021 Russia

Received March 26, 2010

The magnetic properties of the  $\text{EuMn}_2\text{O}_5$  multiferroic (samples consisting of single crystals and ceramic samples) have been investigated by the muon-spin-relaxation ( $\mu\text{SR}$ ) method in the temperature range of 10–300 K. Below the magnetic ordering temperature  $T_N = 40$  K, the loss of the polarization of muons and the effect of the external magnetic field have been observed. Both phenomena can be explained by an additional channel of the depolarization of muons owing to the appearance of muons in a medium with a low electron density due to the charge separation process (the redistribution of the electron density in the phase transition process). The “memory” phenomenon has been revealed in a sample in the external magnetic field; the memory relaxation time depends on the size of the structure units of the samples (single crystals or ceramic grains).

DOI: 10.1134/S002136401010005X

Multiferroics are promising materials for the production of elements of devices transforming magnetic signals into electric ones. This property is due to the large magnetoelectric effect observed in a number of compounds, in particular, in  $\text{RMn}_2\text{O}_5$  manganites (R is a rare-earth element) in which the antiferromagnetic and ferroelectric orders coexist at low temperatures [1, 2]. Their crystal structure corresponds to an orthorhombic lattice and was studied in, e.g., [3].

Most  $\text{RMn}_2\text{O}_5$  manganites have three magnetic subsystems ( $\text{R}^{3+}$ ,  $\text{Mn}^{3+}$ , and  $\text{Mn}^{4+}$ ). One of the exclusions is the  $\text{EuMn}_2\text{O}_5$  compound, where the  $\text{Eu}^{3+}$  ion is nonmagnetic in the ground state, and its magnetic properties are determined only by the  $\text{Mn}^{3+}$  and  $\text{Mn}^{4+}$  ions. A sample is paramagnetic at high temperatures. At the Néel temperature  $T_N = 40$  K, the  $\text{Mn}^{3+}$  and  $\text{Mn}^{4+}$  ions are ordered and a long-range magnetic order appears. The effect of the magnetic scattering of neutrons is observed [4] and, simultaneously with a weak anomaly of the magnetic susceptibility  $\chi$  [5], the temperature dependence of the dielectric constant  $\varepsilon(T)$  has a sharp peak at the temperature  $T_{\text{FE1}} = 35$  K close to the Néel temperature [1, 5, 6]. A shift of the Raman spectrum is also observed in this range [7]. It had been found that these phenomena are due to the ferroelectric transition stimulated by the appearance of the long-range magnetic order at the temperature  $T_N = 40$  K, which results in an additional distortion of the positions of the  $\text{Mn}^{3+}$  ions along the  $a$ -axis. The next phase transition occurs at the temperature  $T_{\text{FE2}} = 22$  K and is accompanied by an increase in the intensity of the magnetic scattering of neutrons [4], a weak

anomaly in the magnetic susceptibility  $\chi$  [1], a sharp peak of the dielectric constant [1, 5, 6], and a jump in the intensity of the passage of millimeter electromagnetic radiation [6]. The analysis of the data indicates that this structure phase transition is initiated by the rotation of the magnetic moments of the  $\text{Mn}^{3+}$  and  $\text{Mn}^{4+}$  ions and by the shift of the  $\text{Mn}^{4+}$  ions along the  $c$ -axis.

A wide anomaly in the temperature dependence of the dielectric constant  $\varepsilon(T)$  was also revealed in the temperature range  $T = 13$ – $23$  K [1, 4–6], which is correlated with the bends in the temperature dependence of the magnetic susceptibility  $\chi(T)$  and with the features of the magnetic scattering of neutrons. These effects can imply the existence of magnetic and structural inhomogeneities.

Unusual phenomena were also revealed at high temperatures (at 100–130 K), but they likely have another nature and are attributed to the existence of limited correlated magnetic regions [5].

The experimental data considered above demonstrate a strong correlation between the electric and magnetic phenomena (magnetoelectric effect) and indicate the relation between the structural and magnetic properties.

In this work, the comparative muon-spin-relaxation ( $\mu\text{SR}$ ) investigation of  $\text{EuMn}_2\text{O}_5$  samples of two types (consisting of single crystals and ceramic grains) is performed in the temperature range of 15–140 K and indicates the qualitative difference between their properties. The time spectra of decay positrons are measured and used to obtain the temperature depen-

dences of the relaxation parameters of the muon polarization, the frequencies of the muon spin precession in the internal magnetic fields of the samples, and the partial contributions of various precession modes to the total asymmetry.

The samples were studied on a setup mounted at the exit of the muon channel of the synchrocyclotron at the Petersburg Nuclear Physics Institute, Russian Academy of Sciences. The setup, the procedure of the measurement of the  $\mu\text{SR}$  spectra, the processing of the spectra, and the procedure of obtaining the relaxation parameters of the muon polarization; the frequencies of the muon spin precession in the internal magnetic fields of the samples; and the partial contributions to the total asymmetry of the muon decay were described in detail in [8, 9]. Polarized  $\mu^+$ -muons having the momentum distribution with a mean momentum of  $p_0 = 90 \text{ MeV}/c$  and a FWHM of  $\Delta p/p = 0.02$  stopped in a target, which was a container with 2–3-mm single crystals randomly oriented with respect to the muon spin or a ceramic sample manufactured by solid-phase synthesis with a diameter of 35 mm and a thickness of about 5 mm. The sample was placed in a cryostat, where the necessary temperature in the range under investigation was maintained with an accuracy of  $\pm 0.2 \text{ K}$ .

The time spectra of decay positrons were measured in long ( $\sim 10 \mu\text{s} \approx 4.5\tau_\mu$ , where  $\tau_\mu = 2.19711 \mu\text{s}$  is the muon lifetime) and short ( $\sim 1.1 \mu\text{s}$ ) ranges with channel steps of 4.9 and 0.8 ns, respectively. These spectra were approximated by the expression

$$N_c(t) = N_0 \exp(-t/\tau_\mu) [1 + a_s G_s(t) + a_b G_b(t)] + B, \quad (1)$$

where  $N_0$  is the normalization constant proportional to the number of detected positrons;  $a_s$  and  $a_b$  are the contributions to the observed decay asymmetry from muons stopped in the sample and the construction elements of the setup, respectively;  $G_s(t)$  and  $G_b(t)$  are the respective polarization relaxation functions; and  $B$  is the contribution from the random coincidence background. The parameter  $a_b$  is determined from the processing of the time spectrum measured in the external magnetic field at the sample temperature below the Néel temperature ( $\sim 25 \text{ K}$ ). The parameter  $a_s$  can depend on the sample temperature if the variation of the temperature is accompanied by the appearance of additional polarization loss channels (e.g., the formation of muonium with the subsequent fast depolarization).

The polarization relaxation function can usually be represented in the form

$$G_s(t) = G_d(t)G_{st}(t). \quad (2)$$

Such a representation is valid beyond the region of critical fluctuations and phase transitions. The dynamic function  $G_d(t) = \exp(-\lambda_d t)$  describes the

average spatial fluctuations of the internal magnetic fields of the sample at large distances (about the muon diffusion length). The form and parameters of the static function  $G_{st}(t)$  are determined by the structure of the sample at a given temperature and, as a result, by the distribution of magnetic fields in regions preferable for the localization of muons after their deceleration in the sample and the end of their thermalization process.

The static relaxation function of the muon polarization for magnets below the temperature  $T_N$  of the paramagnetic–antiferromagnetic transition has the form

$$G_{st}(t) = 1/3 + 2/3 \cos(\Omega t) \exp(-\Delta t), \quad (3)$$

where  $\Omega = 2\pi F$  is the frequency of the muon spin precession in the local magnetic field acting on the muon and  $\Delta$  is the rate of precession damping due to the spread of the local magnetic fields. It is easy to see that in the limiting cases,  $G_{st}(t) = 1$  (in the paramagnetic state) and  $G_{st}(t) \approx 1/3$  (if the sample is in a magnetically ordered state and other depolarization channels are absent) at times  $t \gg 1/\Delta$  when the static relaxation of the polarization can be neglected.

From the processing of the experimental data in the time range  $t = 0.6\text{--}10 \mu\text{s}$ , where the effect of static magnetic fields is negligibly small, the dynamic relaxation rate  $\lambda_d$  and the residual asymmetry  $a_s$  were obtained throughout the temperature range under investigation. The initial asymmetry  $a_0$  was determined from the processing of the measured time spectra of the muon spin precession in the external magnetic field at temperatures  $T > T_N = 40 \text{ K}$  when the sample is paramagnetic. The results are presented in Figs. 1 and 2. The ratio  $a_s/a_0$  is also shown in Fig. 2.

The temperature dependences of the parameter  $\lambda_d$  are the same for both samples and exhibit a sharp peak at the temperature  $T_N \approx 40 \text{ K}$ , which is attributed to the paramagnetic–antiferromagnetic phase transition.

Anomalies in the behavior of  $\lambda_d$  are observed at temperatures of 30 K (FE1 transition) and 22 K (FE2 transition).

The behavior of the residual asymmetry (see Fig. 2) remains almost unchanged above the Néel temperature  $T_N \approx 40 \text{ K}$ . However, the residual asymmetry  $a_s/3$  below the Néel temperature  $T_N$  is much smaller than  $a_0/3$ , indicating the appearance of the additional channel of muon depolarization, e.g., on the formation of long-lived muonium  $\text{Mu}$  (the  $\mu^+e^-$  bound state) in the samples. Muonium is rapidly depolarized and, thus, the observed asymmetry is partially lost. However, for the formation of muonium, it is necessary to change the electron (charge) density. The charge density decreases at the sites where muons prefer to stop. The redistribution of the charge density is

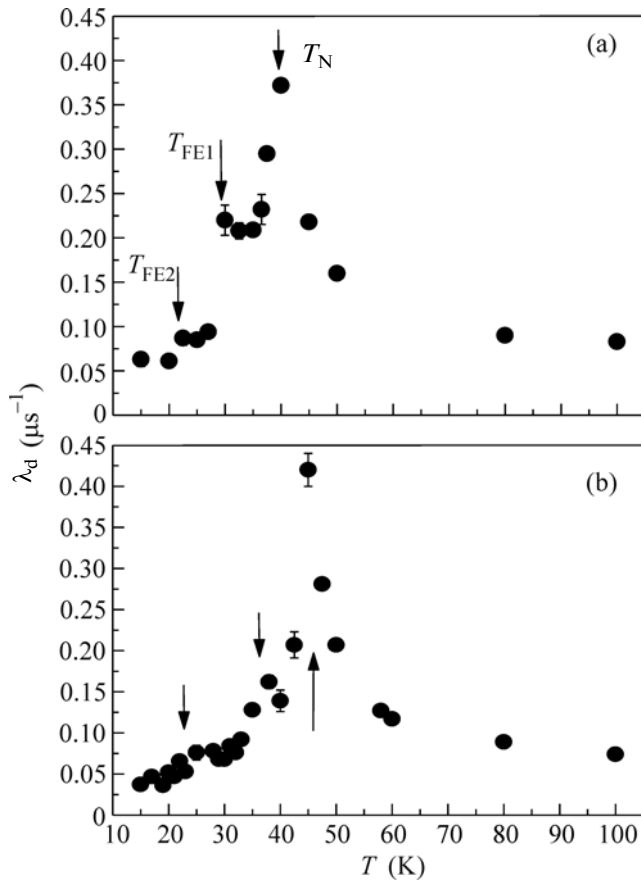


**Fig. 1.** Temperature dependence of the dynamic relaxation of the muon polarization for the (a) sample consisting of single crystals and (b) ceramic sample. The arrows mark the anomalies discussed in the main text.

likely due to the appearance of the internal magnetic field below the temperature  $T_N$  [10].

Both samples exhibit the same behavior of the residual asymmetry almost throughout the temperature range under consideration. Exceptions are the measurements in the external magnetic field and the measurements after the switching-off of the magnetic field.

The residual asymmetry changes significantly in the uniform transverse external magnetic field (at 25 and 30 K for the ceramic sample and sample consisting of single crystals, see Figs. 3 and 4, respectively). The external magnetic field apparently leads to the redistribution of the charge density and to the enhancement of the muonium formation channel [11].

An unusual behavior of the residual asymmetry is observed at the time when the external magnetic field is switched off. The residual asymmetry in the ceramic sample (see Fig. 3) quite rapidly ( $t < 10$  min) reaches the average level. The residual asymmetry in the sample consisting of single crystals (see Fig. 4) decreases at

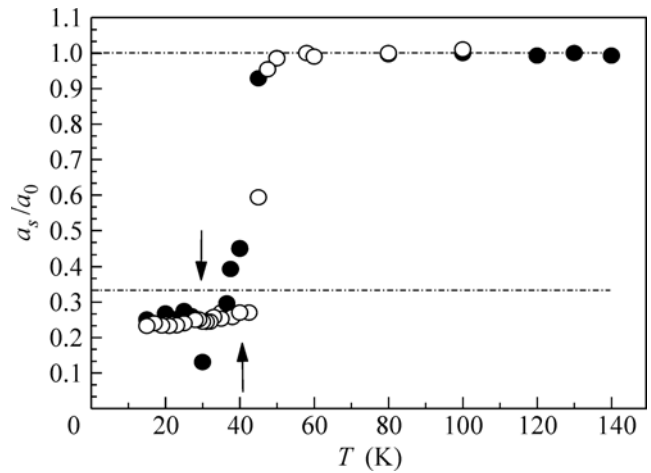


**Fig. 2.** Temperature dependence of the relative residual asymmetry  $a_s/a_0$  for the (closed circles) sample consisting of single crystals and (open circles) ceramic sample. The arrows mark the transition temperature  $T \approx 30$  K for the single-crystal sample and the magnetic ordering temperature  $T_N \approx 40$  K.

the time when the external magnetic field is switched off and returns very slowly (in about 10 h) to the level corresponding to the asymmetry in zero magnetic field.

Figures 5 and 6 show the time evolution of the rate of the dynamic relaxation of the polarization,  $\lambda_d$ , after switching-off the external magnetic field. It is seen that  $\lambda_d$  decreases when the external field is switched on (see Fig. 5). After switching-off the magnetic field in the ceramic sample,  $\lambda_d$  returns almost instantaneously to the average value. In the single crystal sample (see Fig. 6),  $\lambda_d$  increases strongly at the time when the external magnetic field is switched off, then decreases, and reaches the average value. Thus, the effect of “memory” about the action of the external magnetic field on the sample consisting of single crystals exists. The relaxation time of such memory most likely depends on the sizes of the crystals in the sample.

Measurements for the ceramic sample were performed in different sample cooling regimes. In one regime, the temperature is monotonically decreased from the values for the paramagnetic region to low temperatures (60  $\rightarrow$  15 K, open points in Fig. 7). In the other regime, the minimum temperature of 15 K is first established rapidly (in about 1.5 h) and, then, the measurements were performed with a monotonic increase in the temperature (15  $\rightarrow$  60 K, the closed points in Fig. 7). As is seen in Fig. 7, the residual asymmetry depends on the cooling regime. This means that the structural properties of the sample possibly depend on its cooling regime. We emphasize that the observed effect is independent of the sample thermalization time, because the statistics collection time at each

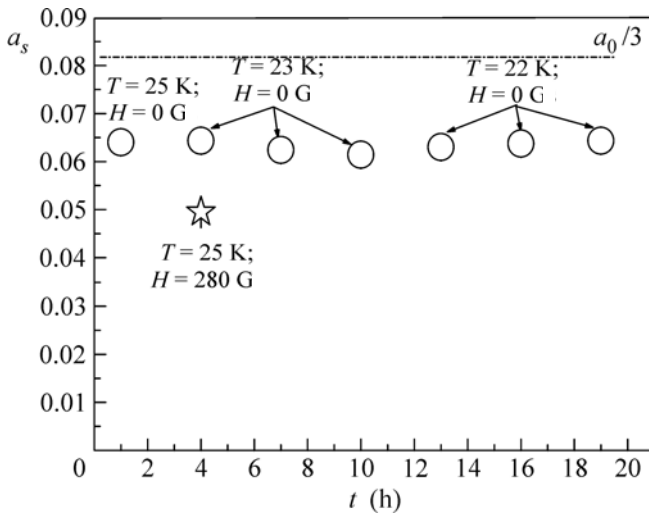


**Fig. 3.** Time dependence of the residual asymmetry  $a_s$  for the ceramic sample in (circles) zero magnetic field and (star) a field of 280 G.

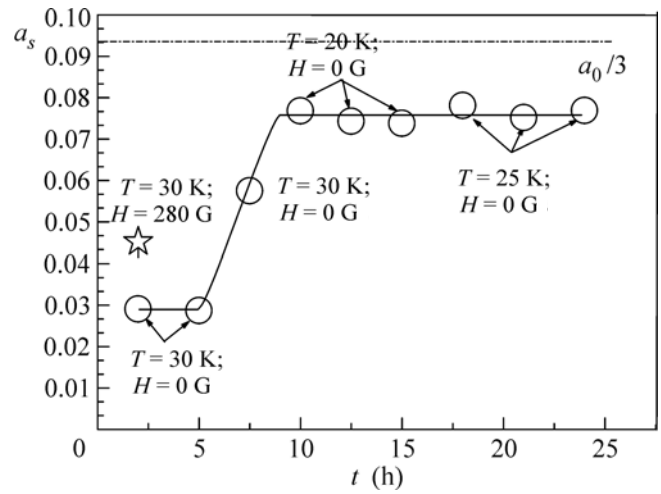


**Fig. 4.** Time dependence of the residual asymmetry  $a_s$  for the sample consisting of single crystals in (circles) zero magnetic field and (star) a field of 280 G.

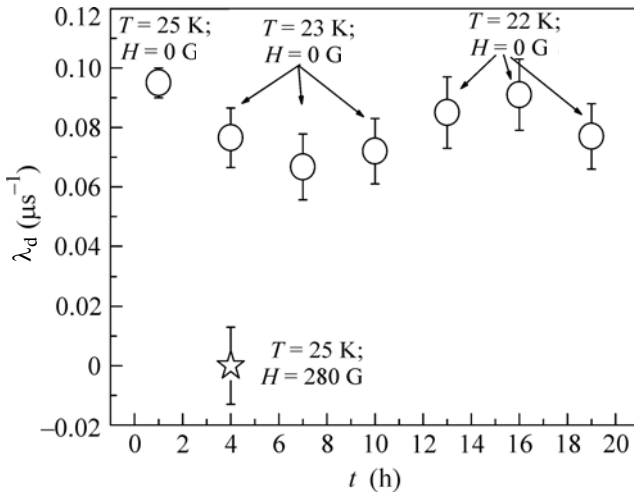


**Fig. 5.** Time dependence of the dynamic relaxation of the muon polarization for the ceramic sample.

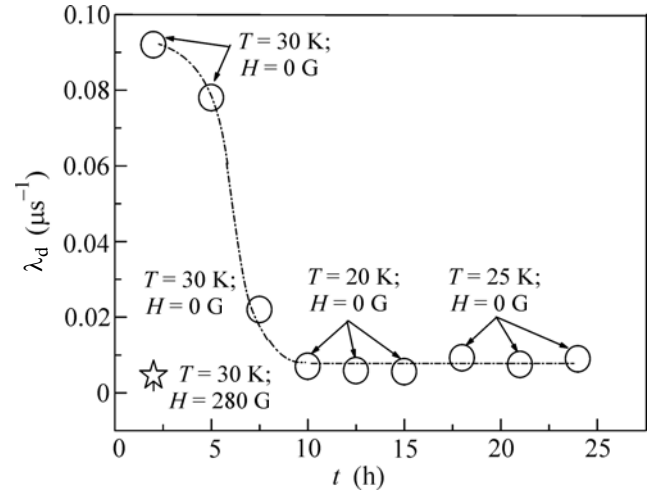


**Fig. 6.** Time dependence of the dynamic relaxation of the muon polarization for the sample consisting of single crystals.

point is several hours (exposition times at each closed and open points were 3 and 8 h, respectively).

Below the Néel temperature  $T_N \approx 40$  K, the long-range magnetic order appears in the samples. The best approximation of the time spectra is obtained with the static relaxation functions in the form

$$a_s G_{st}(t) = a_1 [1/3 + 2/3 \cos(\Omega_1 t) \times \exp(-\Delta_1 t)] + a_2 [1/3 + 2/3 \cos(\Omega_2 t) \exp(-\Delta_2 t)]. \quad (4)$$

The muon spin precession was observed with the angular frequencies  $\Omega_{1,2} = 2\pi F_{1,2}$  (see Figs. 8, 9), frequency spread ( $\Delta_{1,2}$ ), and partial contributions  $a_1$  and  $a_2$  (see Figs. 10 and 11) in the observed residual asymmetry  $a_s = a_1 + a_2$  of the decay of muons stopped in the corresponding samples.

For both samples (consisting of single crystals and ceramic grains), the two frequencies  $F_1$  and  $F_2$  are present in the spectra throughout the temperature range below the Néel temperature  $T_N$ ; the relation between their partial contributions remains almost

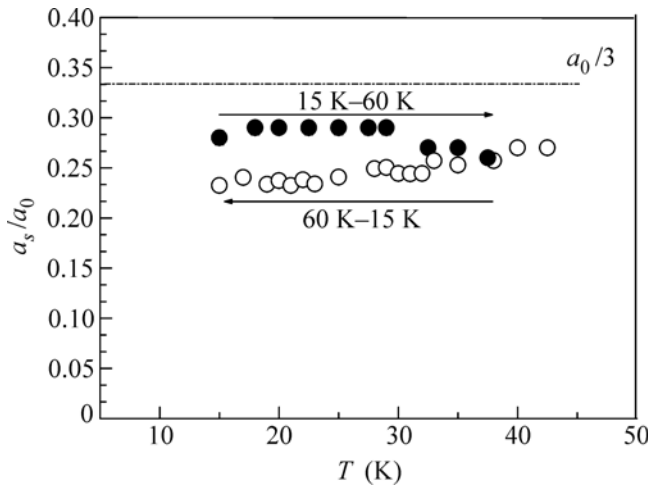


**Fig. 7.** Temperature dependence of the relative residual asymmetry  $a_s/a_0$  for the ceramic sample measured in two sample cooling regimes (for details, see the main text). The arrows indicate the sequence of the measurements.

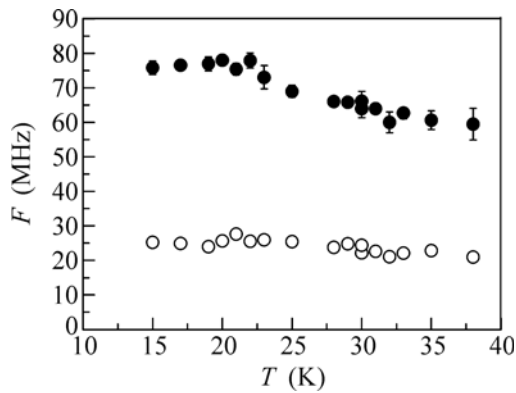


**Fig. 9.** Temperature dependences of the precession frequencies (open circles)  $F_1$  and (closed circles)  $F_2$  of the muon in the internal magnetic field of the ceramic sample.

unchanged (within the errors). The ratio of the observed frequencies ( $F_2/F_1 \approx 3$ ) is constant throughout the temperature range below the magnetic ordering temperature ( $T < T_N$ ). The frequency for the sample consisting of single crystals increases with a decrease in the temperature according to the Curie–Weiss law

$$F_1 = 39(1 - T/T_N)^{0.39} \text{ and } F_2 = 109(1 - T/T_N)^{0.39}.$$

A sharper increase in the frequencies  $F_1$  and  $F_2$  is observed near  $T \approx T_N$  in the ceramic sample.

The phase transitions in the samples at the temperatures  $T_{FE1} \approx 30$  K and  $T_{FE2} \approx 22$  K, which are manifested in the  $\lambda_d(T)$  dependence (see Fig. 1), almost do not affect the behavior of the frequencies  $F_1$  and  $F_2$  and partial asymmetries  $a_1$  and  $a_2$ .

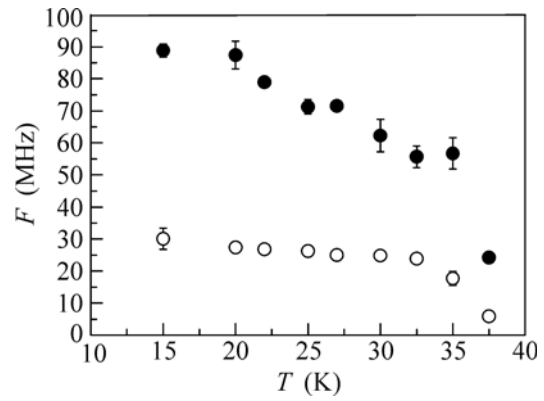


**Fig. 8.** Temperature dependences of the precession frequencies (open circles)  $F_1$  and (closed circles)  $F_2$  of the muon in the internal magnetic field of the sample consisting of single crystals. These dependences correspond to the Curie–Weiss law,  $F_1 = 39(1 - T/T_N)^{0.39}$  and  $F_2 = 109(1 - T/T_N)^{0.39}$ .

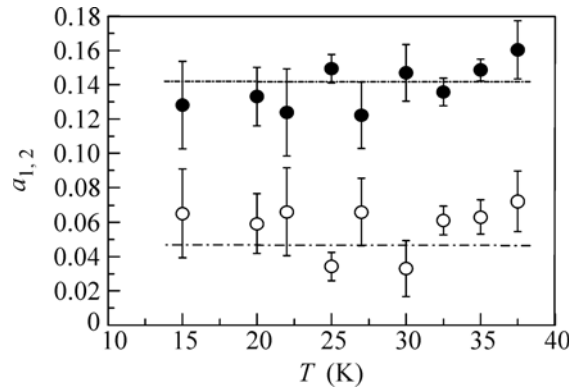


**Fig. 10.** Temperature dependences of the partial contributions (open circles)  $a_1$  and (closed circles)  $a_2$  to the total asymmetry below the Néel temperature  $T_N = 40$  K for the sample consisting of single crystals.

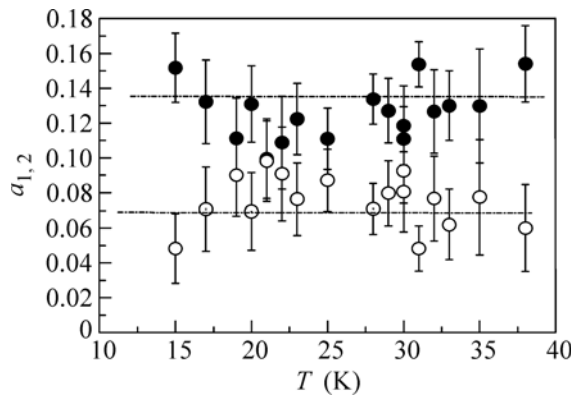


**Fig. 11.** Temperature dependences of the partial contributions (open circles)  $a_1$  and (closed circles)  $a_2$  to the total asymmetry below the Néel temperature  $T_N = 40$  K for the ceramic sample.

## CONCLUSIONS

Thus, the  $\mu\text{SR}$  investigation of  $\text{EuMn}_2\text{O}_5$  multiferroic again demonstrates the efficiency of this method for studying magnetic materials. The  $\mu\text{SR}$  investigation of two  $\text{EuMn}_2\text{O}_5$  samples (consisting of single crystals and ceramic grains) has revealed a number of interesting features of this compound.

(i) The charge density changes locally in both samples at the temperatures  $T < T_N$ ; this change is manifested in the additional depolarization of muons.

(ii) The external magnetic field also leads to the loss of the polarization in the samples at  $T < T_N$  and likely gives rise to the additional redistribution of the charge density in the samples.

(iii) The effect of “memory” about the action of the external magnetic field has been observed in the samples. The relaxation time of this memory depends on the sizes of the structural units (single crystals and ceramic grains).

(iv) The phase transitions observed at the temperatures  $T < T_N$  are not manifested in the distribution of the internal local magnetic fields. They are seen only in the temperature dependence of the dynamic relaxation rate  $\lambda_d(T)$ .

(v) The electron density is redistributed at the phase transition point at the temperature  $T_N$ . The mechanism of multiferroicity is possibly associated with this phenomenon.

A further investigation of such samples with various sizes of the structure units is of interest. An interesting question is whether the polarization loss effect exists in other manganites, e.g.,  $\text{RMnO}_3$ , or this is a feature of

the  $\text{RMn}_2\text{O}_5$  compound with two manganese ions with different valences.

## REFERENCES

1. E. I. Golovenchits, N. V. Morozov, V. A. Sanina, and L. M. Sapozhnikova, *Fiz. Tverd. Tela* **34**, 108 (1992) [*Sov. Phys. Solid State* **34**, 56 (1992)].
2. H. Tsujino and K. Kohn, *Solid State Commun.* **83**, 639 (1992).
3. P. G. Radaelli and L. C. Chapon, *J. Phys.: Condens. Matter* **20**, 434213 (2008).
4. V. Polyakov, V. Plakhty, M. Bonnet, et al., *Physica B* **297**, 208 (2001).
5. E. I. Golovenchits, V. A. Sanina, and A. V. Babinskii, *Zh. Eksp. Teor. Fiz.* **112**, 284 (1997) [*JETP* **85**, 156 (1997)].
6. V. A. Sanina, L. M. Sapozhnikova, E. I. Golovenchits, and N. V. Morozov, *Fiz. Tverd. Tela* **30**, 3015 (1988) [*Sov. Phys. Solid State* **30**, 1736 (1988)].
7. A. F. Garsia-Flores, E. Granado, H. Martinho, et al., *Phys. Rev. B* **73**, 104411 (2006).
8. S. G. Barsov, S. I. Vorob'ev, V. P. Koptev, et al., *Prib. Tekh. Eksp.* **50** (6), 36 (2007) [*Instrum. Exp. Tech.* **50**, 750 (2007)].
9. S. G. Barsov, S. I. Vorob'ev, E. N. Komarov, et al., Preprint PIYaF No. 2738 (Gatchina, 2007).
10. V. A. Sanina, E. I. Golovenchits, and V. G. Zaleskii, *Fiz. Tverd. Tela* **50**, 874 (2008) [*Phys. Solid State* **50**, 913 (2008)].
11. S. G. Barsov, S. I. Vorob'ev, E. I. Golovenchits, et al., *Soobshch. PIYaF* No. 2826 (Gatchina, 2009).

*Translated by R. Tyapaev*